



**What can pKa and NBO charges of the ligands tell us about
the water and thermal stability of Metal Organic
Frameworks?**

Journal:	<i>Journal of Materials Chemistry A</i>
Manuscript ID:	TA-ART-06-2014-003154
Article Type:	Paper
Date Submitted by the Author:	21-Jun-2014
Complete List of Authors:	<p>Lu, Ping; Nanjing Normal University, School of Chemistry and Materials Science Wu, Yong; Nanjing Normal University, School of Chemistry and Materials Science Kang, Hong; Nanjing Normal University, School of Chemistry and Materials Science Wei, Haiyan; Nanjing Normal University, Jiangsu Key Laboratory of Biofunctional Materials, School of Chemistry and Materials Science Liu, Hong-Ke; Nanjing Normal University, Jiangsu Key Laboratory of Biofunctional Materials, School of Chemistry and Materials Science; Nanjing University, State Key Laboratory of Coordination Chemistry Fang, Min; Nanjing Normal University, School of Chemistry and Materials Science; Nanjing Normal University, Jiangsu Key Laboratory for NSLSCS; Nanjing University, State Key Laboratory of Coordination Chemistry</p>

What can pK_a and NBO charges of the ligands tell us about the water and thermal stability of metal organic frameworks?

Ping Lu,^a Yong Wu,^a Hong Kang,^a Haiyan Wei,^{*b} Hongke Liu,^{b,d} Min Fang^{*a, c, d}

^a Department of Chemistry, School of Chemistry and Material Science, Nanjing Normal University, Nanjing 210023, China

^b Jiangsu Key Laboratory of Biofunctional Materials, School of Chemistry and Material Science, Nanjing Normal University, Nanjing 210023, China

^c Jiangsu Key Laboratory for NSLSCS, Nanjing Normal University, Nanjing 210023, China

^d State Key Laboratory of Coordination Chemistry, Nanjing University, Nanjing 210093, China

Email addresses of corresponding authors: fangmin@njnu.edu.cn (M. Fang), weihaiyan@njnu.edu.cn (H. Wei)

Abstract

Hydrothermal stability of metal organic frameworks (MOFs) is critical for their application for hydrogen storage and other applications. The pK_a^1 values of the conjugated acids of ligands and natural bond orbital (NBO) charges of the coordinating atoms of 32 multicarboxylate ligands and 31 N-heterocyclic ligands applied in the MOF syntheses were calculated at 298.15 K with B3LYP/6-31+G(d,p) level of calculations. Solvation Gibbs energies (ΔG_{solv}) in aqueous solution are obtained using SMD modeling. NBO charges were calculated based on optimized structures in gas phase. We found the calculated pK_a^1 values have linear relationship with the experimental results of a few known bidentate ligands, but pK_a^2 values do not. We demonstrated that NBO charges of the coordinating atoms of the ligands, like pK_a^1 values of the conjugated acids of the ligands, can reflect the relative coordination abilities of the ligands to metal ions and the strength of the resulted M-L bonds. To our knowledge, systematic calculations of the pK_a values and NBO charges of multidentate ligands have not been reported. Our work provides relative comparisons of the coordination abilities of these ligands and the calculation method can be applied to new ligands. Some experimental results about water and thermal stability of MOF materials were successfully explained in terms of M-L bond strengths and polarity based on our calculated results. The results can be used to predict whether a targeted MOF structure would be water and thermally stable, predict the hydrothermal stability of known MOFs, design new hydrothermally stable MOFs and provide guidance for the synthetic procedures based on the calculated pK_a values. The limitations of applying these values were also given.

1. Introduction

The world is facing the problem of energy shortage and pollution due to an economy heavily relied on petroleum. An economy based on hydrogen might alleviate this problem. One of the key issues for the application of H₂ is its efficient storage for fuel cell applications. Various hydrogen storage methods were studied, including high pressure tanks, metal hydrides and hydrogen adsorption,¹ among which hydrogen adsorption using MOF materials was considered one of the most promising method. Extensive works on the hydrogen storage using MOFs were carried out and many review papers have been published,² including works by spillover methods.³

MOFs were first reported in 1989,⁴ referring to a class of crystalline compounds with infinite porous 2D or 3D network structures assembled from organic ligands and metal ions or small metal-containing clusters.⁵ MOFs have attracted tremendous attention over the past years.⁵ Compared with other type porous materials, their synthetic procedures are easy, and they can have very high specific surface area (BET: 4500-6000 m²/g) and low density (0.25-0.38 g/cm³), as well as tunable pore size and functionality.⁶ Water and thermal stability of MOFs are critical for the hydrogen storage application. But many MOF materials are sensitive to water molecules in the air, limiting their practical applications.⁷ For example, the known MOF-5 was found unstable in air due to its sensitivity to moisture.⁸ In practical production, it is very difficult to get rid of the water in hydrogen gas completely, and the additional cost to remove water is also very high. Therefore making MOFs with high water stabilities are essential for their application for hydrogen storage.

There have been some reports about the water stability of MOFs. Willis et al.⁹ studied hydrothermal stability of 10 MOFs both experimentally and through quantum mechanical calculations. Their work suggests that the strength of the bond between the metal oxide cluster and the bridging linker is important in determining the hydrothermal stability of the PCP (Porous Coordination Polymer). They also found the structures of the secondary building units (SBUs) have influence on the hydrothermal stability. They proposed that the MOFs containing 6-coordinate metal ions tend to be more water stable than those containing 4-coordinate metal ions due to steric effect. Through quantum mechanical calculations, they

found the predicted energies for hydrolysis and ligand displacement are uncorrelated and predicted activation energies for ligand displacement by H₂O correlate with the observed hydrothermal stabilities, suggesting that hydrothermal stability of these MOFs is under kinetic control. Walton et al.¹⁰ studied the water stability of pillared MOFs by ligand functionalization. They proposed that the integration of polar functional groups (e.g., nitro, bromo, chloro, hydroxy, etc.) on the dicarboxylate linker renders these MOFs water unstable compared to the parent MOF and placing nonpolar groups (e.g., methyl) on the terephthalate (BDC²⁻) ligand results in structurally robust MOFs. Pyrazole class of MOFs shows high stability in boiling water and other chemical agent.¹¹ ZIF-8 is stable up to 10 days, but its structure will change after 3 months in water.¹² Kaskel et al.⁷ found that both HKUST-1 and DUT-4 turned out to be unstable in direct contact with water, whereas the MIL-materials do show stability. Researchers found that the thermal stability and water stability of Zr-MOFs are very high.^{13,14} Zaworotko et al.¹⁵ synthesized two thermodynamically stable MOFs, [M(bpe)₂(M'O₄)] (M = Co or Ni; bpe = 1,2-bis(4-pyridyl)ethene; M' = Mo or Cr), which retain crystallinity even when immersed in water for months, boiling water for 1 day, or 0.1 N NaOH for a week.

We surmise that the pK_a values of the conjugated acids of ligands and natural bond orbital (NBO) charges (the electron densities calculated by the NBO program¹⁶) of the coordination atoms of ligands can possibly reflect their coordination ability of the ligands to metal ion, and stronger coordination ability contributes to high thermal and water stability due to the formation of stronger metal-ligand (M-L) bonds. Some papers also proposed that the stability of MOFs has something to do with the pK_a values of the conjugated acids of the ligands.^{11,17} We think such information is important for developing design criteria for future synthetic efforts. Many groups have calculated the pK_a values of monocarboxylic acids¹⁸ and some organic bases.¹⁹ Fabian et al.²⁰ used ab initio (MP2) and DFT (B3LYP) method combined with the 6-31G(d,p) and 6-31+G(d,p) to predict the pK_a values of seleninic, selenenic, sulfinic and monocarboxylate acids. However, it is usually multicarboxylate ligands which are used to synthesize the MOFs. However, only a few experimental pK_a values are available for multicarboxylic acids and N-H containing heterocyclic compounds which are applied in MOF syntheses. The calculation of pK_a values of multicarboxylic acids and N-H containing

heterocyclic compounds is lacking. Tae Bum Lee and Michael L. McKee²¹ studied the dependence of pK_a values on different models of solute cavities by calculating some simple diprotic and triprotic acids based on DFT/aug-cc-pVTZ combined with CPCM or SMD solvation modeling.

In this work, we systematically calculated NBO charges (gas phase) and/or the pK_a^1 values (in aqueous solution, conjugated acids of the ligands) of 32 multicarboxylate ligands and 31 N-containing heterocyclic ligands using DFT at the B3LYP/6-31+G(d,p) level of theory. Solvation Gibbs energies (ΔG_{solv}) in aqueous solution are obtained using SMD modeling. We demonstrated that the calculated pK_a^1 values and experimental data have a good linear relationship for 9 multicarboxylic acids and 4 N-H containing heterocyclic compounds. We can therefore predict the relative coordination strengths of ligands which have no experimental values in right order based on calculated pK_a^1 values. Thus, our work makes it possible to make comparisons of the coordination abilities of many commonly used multicarboxylate and N-containing ligands for the first time. We successfully explained the water and thermal stabilities of some MOF materials in terms of M-L bond strengths and bond polarity. In addition, we found NBO charges, like pK_a^1 values can be used to predict M-L bond strengths so that can be used to predict the stability of MOFs. Our calculated results Based on our calculated results which can be easily extended using the easy and not costly calculation method can help to design new stable MOFs, predict water stability of known MOFs, and give guidance for the synthetic procedures.

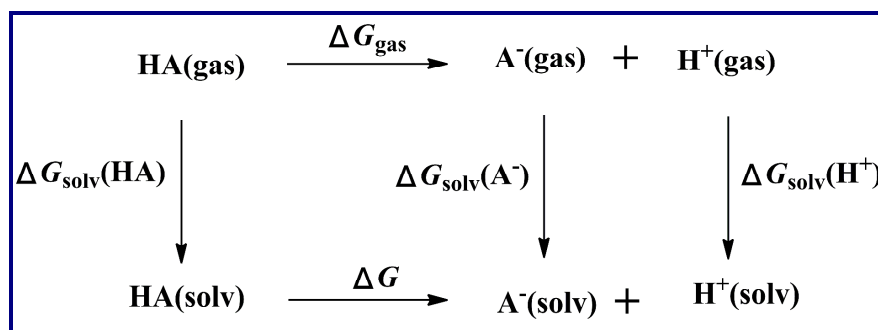
2. Computational details

All geometry optimizations and vibrational analyses were performed with the Gaussian 09. Gas phase geometries of both neutral and anionic species in Table 1 were optimized using DFT at the B3LYP/6-311++G(d,p) and B3LYP/6-31+G(d,p) level of theory. All calculated structures are true minima, i.e., no imaginary frequencies were observed. The zero-point vibrational energy, thermal corrections (298 K), and the entropy term were added to the electronic energy to provide the free energy. Solvation Gibbs energies (ΔG_{solv}) in water are obtained using SMD developed by the Truhlar/Cramer group,²² which is the recommended choice for computing ΔG of solvation in Gaussian 09. Examples of input files for the

calculations are given in Supporting Information.

We applied the B3LYP/6-31+G(d,p) level of theory to calculate the NBO charges of the coordination atoms of these ligands (completely deprotonated ligands) based on calculated gas phase geometries. The calculations of pK_a values usually employ thermodynamic cycles.²³ Here we applied a standard thermodynamic cycle named Born-Haber cycle (scheme 1 and eq 1, 2 and 3).²⁴

SCHEME 1



$$pK_a = \Delta G_{\text{solv}}/2.303 RT \quad (1)$$

$$\Delta G_{\text{solv}} = \Delta G_{\text{gas}}(1 \text{ M}) + \Delta G_{\text{solv}}(A^-) + \Delta G_{\text{solv}}(H^+) - \Delta G_{\text{solv}}(HA) \quad (2)$$

$$\Delta G_{\text{gas}}(1 \text{ atm}) = G_{\text{gas}}(A^-) + G_{\text{gas}}(H^+) - G_{\text{gas}}(HA) \quad (3)$$

The values for $G_{\text{gas}}(H^+)$ and $\Delta G_{\text{solv}}(H^+)$ are derived from experiment. We used the values $G_{\text{gas}}(H^+) = -6.28 \text{ kcal mol}^{-1}$. The value of $\Delta G_{\text{solv}}(H^+)$ was under debate in the literature for some time, but the value now generally accepted is $-265.9 \text{ kcal/mol}^{-1}$.^{23a, 24-25} The calculation of ΔG_{gas} uses a reference state of 1 atm and the calculation of ΔG_{solv} uses a reference state of 1 M. Converting the ΔG_{gas} reference state (22.46 L at 298.15 K) from 1 atm to 1 M is accomplished using equation 4. Based on equation 1-4, the pK_a values using the thermodynamic cycle are derived as shown in equation 5.^{24a}

$$\Delta G_{\text{gas}}(1 \text{ M}) = \Delta G_{\text{gas}}(1 \text{ atm}) + RT \ln(24.46) \quad (4)$$

$$pK_a = [G_{\text{gas}}(A^-) - G_{\text{gas}}(HA) + \Delta G_{\text{solv}}(A^-) - \Delta G_{\text{solv}}(HA) - 270.28]/1.364 \quad (5)$$

3. Results and discussion

3.1 Why do we calculate pK_a and NBO charges?

pK_a values indicates the acidity of an acid. Smaller the pK_a value is, stronger the acidity of the acid. The basicity of the conjugated base of a stronger acid is weaker than that of the

conjugated base of a weaker acid. According to Lewis acid-base theory, the basicity is the ability of giving electrons. This explains that a stronger base will form a stronger M-X bond and thus will result in a more stable MOF, which has been also proposed by others and supported by experimental evidence.^{11, 17}

A strong base usually has high electron density on the atoms which are to give electrons and are the coordinating atoms. We therefore think the electron density (i.e. the negative charges) on the coordinating atom of the conjugated base might also reflect its ability of forming an M-X bond. In this work, the electron densities were calculated by the NBO scheme implemented by the Gaussian 09 software¹⁶

Ligands with N or O coordinating atoms are hard base and the metal ions used in MOFs are usually hard (Be^{2+} , Mg^{2+} , Ca^{2+} , Sc^{3+} , Al^{3+} , Ga^{3+} , Cr^{3+} , Co^{3+} , Fe^{3+} , Ti^{4+} , Zr^{4+} , Ln^{3+}) or border line acids (Mn^{2+} , Fe^{2+} , Co^{3+} , Ni^{2+} , Cu^{2+} , Zn^{2+} , Pb^{2+} , Sn^{2+}).²⁶ Thus ionic bonding should dominate the M-X (X= O or N) bond strength of these metals. Andersen and Bergman et al.²⁷ found the correlation between H-X and Ni-X bond energies (Ni-CF_3 (96.5 kcal/mol) > Ni-F (92.7 kcal/mol) > NiMe (92.0 kcal/mol) > NiOMe (91.4 kcal/mol) > NiNMe₂ (90.4 kcal/mol)) shows a marked preference for nickel binding to more electronegative ligands. They concluded that there is a large electrostatic component in the bonding between Ni and X. N or O atoms with higher electron densities will contain more negative charges, and thus form stronger ionic bonds than those atoms with less electron densities.

The preference for electronegative ligands occur throughout transition metal chemistry, even for soft metal ions.²⁷⁻²⁸ This is because these metal orbital will form stronger covalent bonds with the orbitals of more electronegative ligands.^{28d} More electronegative ligands would contain more electron densities on the coordinating atoms since electronegativity is the ability to obtain electrons. Thus, for the soft acids (Cd^{2+} , Cu^+ , Ag^+ , Au^+ , Pd^{2+} , Pt^{2+} , Hg^{2+}), NBO charges of N or O atoms can also be applied. For example, we can predict a ligand with more NBO charges at the coordinating atom will form a stronger bond with Cd^{2+} than a ligand of the same type but with less NBO charges.

3.2 Calculation method and the calculated results

First we used B3LYP/6-311++G (d,p) combined with SMD to calculate the pK_a^1 and pK_a^2

of 9 dicarboxylic acids, whose pK_a^1 and pK_a^2 values have been experimentally determined. The diffuse basis sets have been chosen since it is recommended for anions and molecules with lone pair electrons.²⁹ The calculated results are given in Table 1 together with the corresponding experimental values. Plotting all of the predicted pK_a values against the experimental data, two straight regression lines were obtained for pK_a^1 and pK_a^2 . The calculated pK_a^1 value and experimental data have a good linear relationship (see Fig. 1a) (the coefficient: 0.9837, the standard deviation: 0.15 unit, the mean absolute deviation (MAD) of pK_a values: 2.36). Since ligands used in the MOFs usually have many atoms, to reduce the cost, we also used B3LYP/6-31+G (d,p) combined with SMD to carry out the above calculations. The values are also listed in Table 1. The calculated pK_a^1 value and experimental data also have a good linear relationship, and the coefficient (0.9918) is even higher than that obtained using 6-311++G (d,p) basis set, the standard deviation is 0.11 unit (Fig. 1c), and the mean absolute deviation (MAD) of pK_a^1 values are 2.42, only slightly higher than the 2.36 using higher basis sets. Although the MAD of 2.42 is bigger than those of related work (MAD: 1.5-2.0).^{20-21, 24b} However these works applied more costly basis sets and/or computation method. The linearity between the calculated and experimental results means that we could predict the right order of the acidities of ligands based on calculated results, which is the purpose of this work. But the calculated pK_a^2 values are unsatisfactory. Although the MAD for pK_a^2 values is smaller (1.51 (higher basis sets)-1.54), the calculated values do not correlate with the experimental values linearly. Thus, the calculated pK_a^2 values cannot be used to predict the acidity order of the ligands. Since pK_a^1 values alone can reflect the coordination strength of the conjugated bases, we can compare their coordination strengths in right order based on calculated pK_a^1 values. Applying 6-31+G(d,p) basis sets, we also calculated pK_a values of 4 N-H containing heterocyclic compounds which having experimental values^{17a} (Table 2). The calculated values also have good correlation with the experimental values as shown in Fig. 2 (the coefficient: 0.9924, sd: 1.1, MAD: 0.91). We therefore choose the 6-31+G (d,p) basis set to do the rest of the calculations and the results are given in Table 3. In addition, we calculated the NBO charges of the coordinating atoms of the ligands. To simplify the situation, we calculated the NBO charges of the completely deprotonated ligands, which are also most commonly found in the MOF structures.

Table 1 Calculated and experimental pK_a values of selected dicarboxylic acids and NBO charges of the coordinating atoms of the corresponding dicarboxylate ligands.

No.	Chemical structure of the dicarboxylate ligands	pK _a (exp.)*		6-311++G(d,p)		6-31+G(d,p)		NBO
		pK _a ¹	pK _a ²	pK _a ¹ (cal.)	pK _a ² (cal.)	pK _a ¹ (cal.)	pK _a ² (cal.)	
1		1.80	4.01	1.04	4.87	0.38	4.96	-0.842
2		3.02	4.38	4.07	5.56	4.02	5.59	-0.815
3		3.51	4.28	5.25	5.93	5.34	6.04	-0.798
4		3.54	4.60	5.63	6.08	5.75	6.17	O1: -0.810 O2: -0.785
5		3.09	4.75	4.10	7.43	4.33	7.33	O1: -0.812 O2,O3:-0.808 O4: -0.819
6		3.85	5.45	7.40	6.49	7.42	6.50	O1: -0.797 O2: -0.814 O3: -0.827 O4: -0.824
7		4.32	5.42	8.15	7.61	8.01	7.56	O1: -0.826 O2: -0.815
8		4.13	5.64	7.19	7.01	7.20	6.99	O1: -0.830 O2: -0.824 O3: -0.829

9		4.21	5.64	8.33	6.77	7.94	6.90	O4: -0.816	
									O1: -0.834
									O2: -0.825
MAD		2.36	1.51	2.42	1.54				

* The experimental pK_a values were taken from the 87th CRC Handbook of Chemistry and Physics.

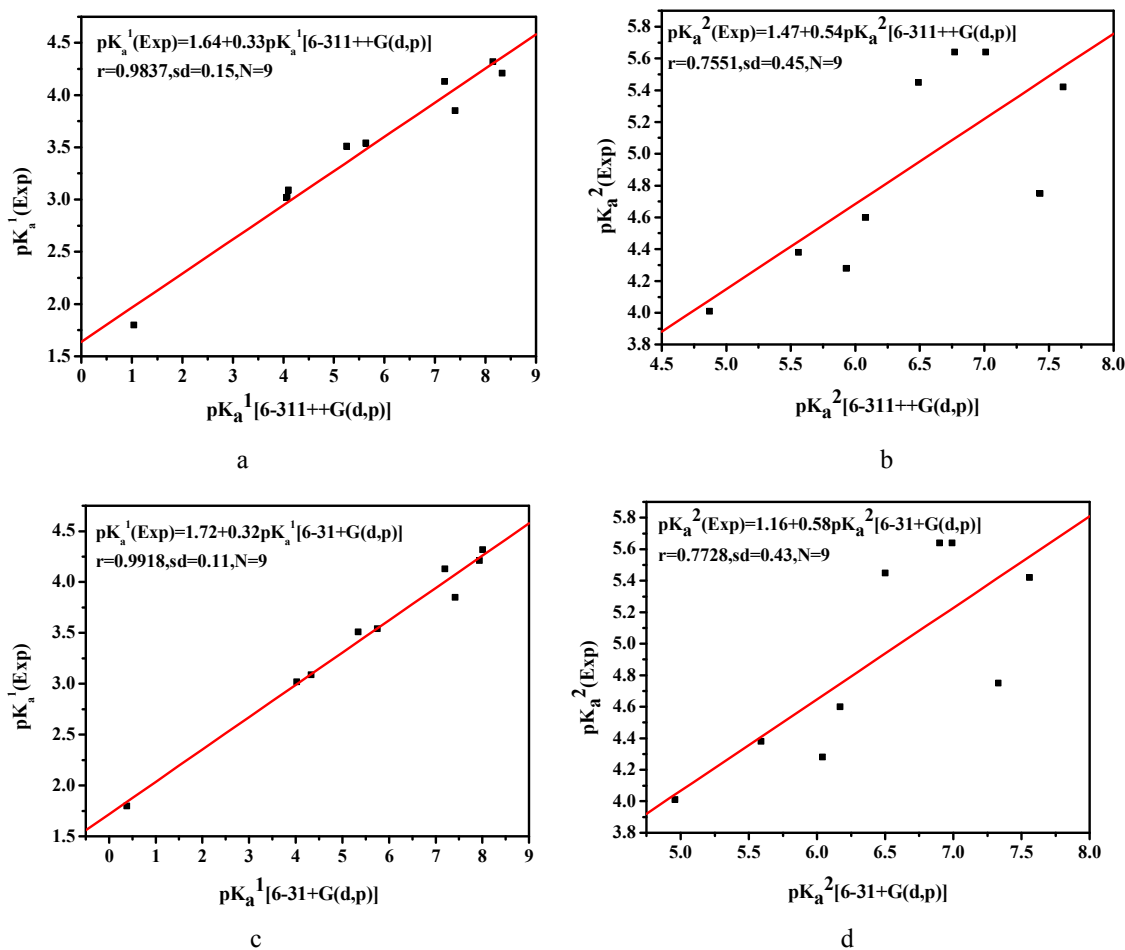
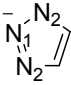
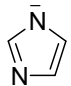
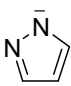


Fig. 1 Correlation between the experimental and theoretical pK_a^1 and pK_a^2 values using different basis sets

Table 2 Calculated and experimental pK_a values of selected N-H containing heterocyclic compounds

No.	Chemical structure	$pK_a(\text{exp.})$	$pK_a(\text{cal.})$	NBO
10		4.9	6.42	N1: -0.417 N2: -0.194

11		13.6	12.47	N1: -0.202 N2: -0.389
12		18.6	17.99	N: -0.512
13		19.8	19.42	N: -0.402
MAD			0.91	

The experimental pK_a values are taken from ref 17a.

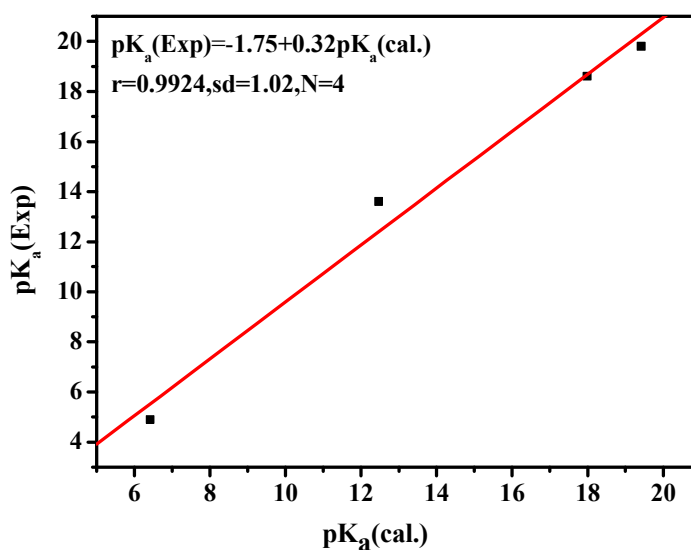
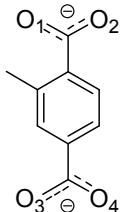
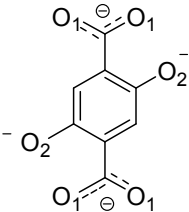
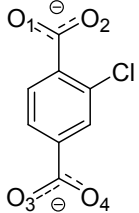
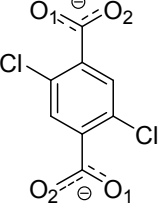
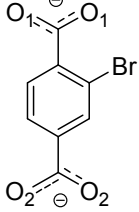
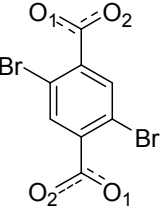
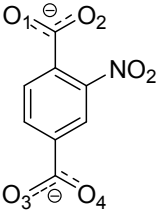
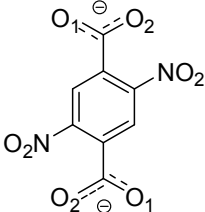


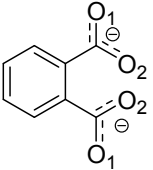
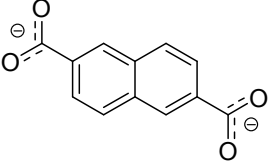
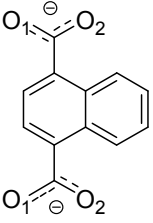
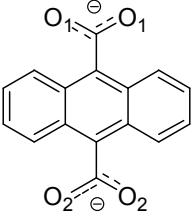
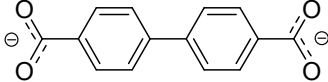
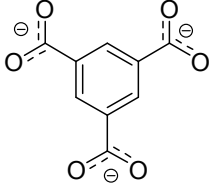
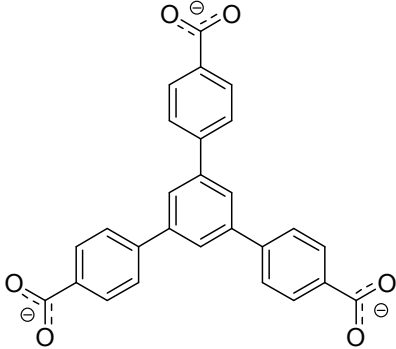
Fig. 2 Correlation between the experimental and theoretical pK_a 's

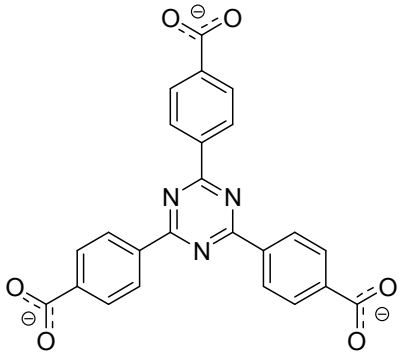
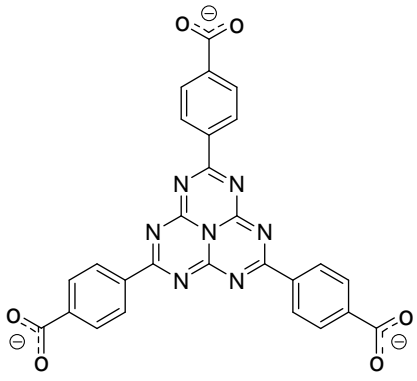
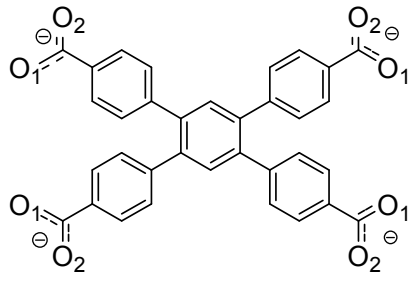
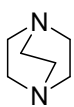
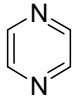
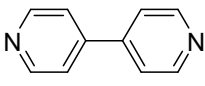
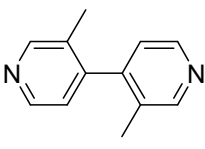
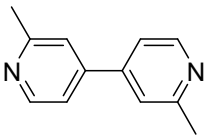
Table 3 The pK_a values (of the conjugated acids of the ligands) and NBO charges of the coordination atoms of selected ligands for MOFs

No.	Ligand structures	pK_a^1	pK_a^2	NBO*
14		4.67	7.04	O1: -0.795 O2: -0.798 O3: -0.797 O4: -0.797

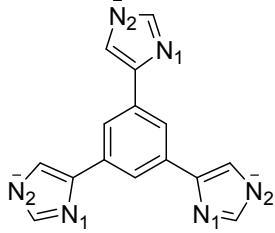
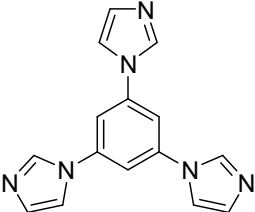
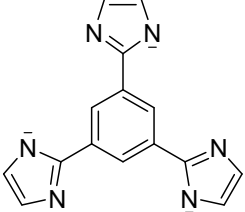
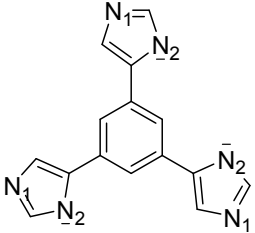
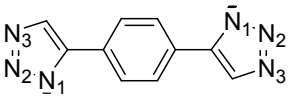
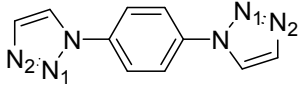
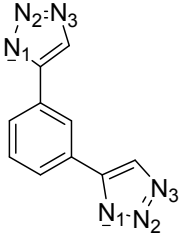
15		3.72	7.20	O1: -0.794 O2: -0.799
16		6.74	5.09	-0.787
17		8.81	7.67	-0.804
18		7.36	7.93	-0.818
19	<p>19a</p> <p>19b</p>	4.79	6.64	O1: -0.791 O2: -0.777 O3: -0.793 O4: -0.802
20	<p>20a</p>	4.16	7.31	O1: -0.805 O2: -0.770

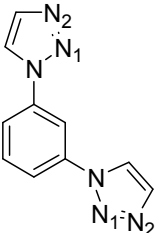
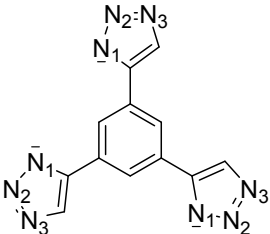
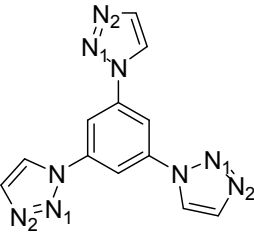
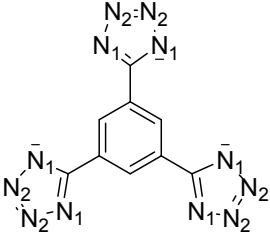
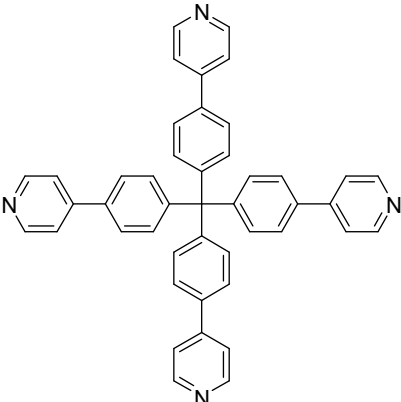
	 <p>20b</p>	pK_a^3 12.20	pK_a^4 26.67	O1: -0.851 O2: -0.936
21		2.53	5.70	O1: -0.779 O2: -0.768 O3: -0.793 O4: -0.795
22		1.83	4.28	O1: -0.763 O2: -0.779
23		1.83	5.72	O1: -0.769 O2: -0.793
24		1.29	9.12	O1: -0.761 O2: -0.786
25		1.69	5.20	O1: -0.778 O2: -0.766 O3: -0.792 O4: -0.786
26		0.52	3.28	O1: -0.771 O2: -0.753

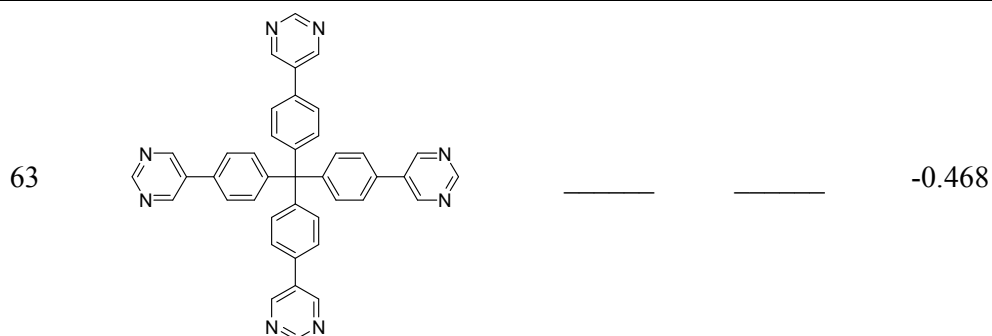
27		5.54	6.09	O1: -0.803 O2: -0.764
28		5.97	6.26	-0.790
29		4.04	7.68	O1: -0.787 O2: -0.790
30		3.96	4.55	O1: -0.797 O2: -0.774
31		3.91	9.02	-0.788
32		4.99	_____	-0.813
33		6.72	_____	-0.788

34		5.85	_____	-0.785
35		5.67	_____	-0.779
36		6.80	_____	O1: -0.789 O2: -0.790
37		_____	_____	-0.522
38		_____	_____	-0.418
39		_____	_____	-0.449
40		_____	_____	-0.447
41		_____	_____	-0.462

42		_____	_____	-0.453
43		18.15	19.66	-0.403
44		17.20	17.94	N1: -0.615 N2: -0.587
45		_____	_____	-0.485
46		18.43	18.33	-0.388
47		18.15	19.27	-0.402
48		17.83	17.14	N1: -0.617 N2: -0.568
49		_____	_____	-0.484
50		18.06	_____	-0.424

51		18.74	—	N1: -0.583 N2: -0.636
52		—	—	-0.479
53		16.77	—	-0.583
54		18.74	—	N1: -0.636 N2: -0.582
55		11.49	12.53	N1: -0.363 N2: -0.201 N3: -0.393
56		—	—	N1: -0.075 N2: -0.246
57		11.51	12.51	N1: -0.364 N2: -0.202 N3: -0.392

58		—	—	N1: -0.077 N2: -0.246
59		11.10	—	N1: -0.358 N2: -0.223 N3: -0.412
60		—	—	N1: -0.069 N2: -0.240
61		5	—	N1: -0.389 N2: -0.215
62		—	—	-0.454



*NBO charges are calculated for the completely deprotonated ligands.

3.3 pK_a^1 values versus NBO charges

To check whether the calculated pK_a^1 values of the conjugated acids of the ligands and NBO charges of the coordinating atoms of the ligands predict the same order of coordination ability of ligands, we chose H_2BDC related species from Table 3 and tabulated the calculated values in Table 4 sorted by the pK_a^1 values. Short names are given for the structures of the conjugated bases.

Table 4 Consistency of calculated pK_a^1 values with NBO charges of the coordinating atoms of the conjugated bases

Short Names	No.	pK_a^1	NBO charges	
$(CH_2)_2BDC$	17	8.810	-0.804	
H_4 -BDC	18	7.360	-0.818	
BTTB	36	6.800	-0.790	
$BDC-(CH_3)_4$	16	6.740	-0.787	
BTB	33	6.720	-0.788	
NDC	28	5.970	-0.790	
N-BTB	34	5.850	-0.785	
NN-BTB	35	5.670	-0.779	
<i>m</i> -BDC	4	5.630	-0.785	-0.810
<i>o</i> -BDC	27	5.540	-0.764	-0.801
BDC	3	5.340	-0.798	
BTC	32	4.990	-0.813	
BDC-OH	19a	4.790	-0.777 ^a	-0.795 ^b
BDC- CH_3	14	4.670	-0.795 ^a	-0.797 ^b
BBDC	31	3.910	-0.788	
$BDC-(CH_3)_2$	15	3.720	-0.794	-0.799
BDC-Cl	21	2.530	-0.768 ^a	-0.789 ^b
BDC-Cl ₂	22	1.830	-0.763	-0.779
BDC-Br	23	1.830	-0.769 ^a	-0.793 ^b

BDC-NO ₂	25	1.690	-0.766 ^a	-0.785 ^b
BDC-Br ₂	24	1.290	-0.761	-0.786
BDC-(NO ₂) ₂	26	0.520	-0.753	-0.771

a. The NBO charge of the O atoms which is nearest to the substituent. b. The average of the NBO charges of the rest O atoms.

We found the trend is when pK_a^1 increases, the NBO charge generally increases. However, there are exceptions. NBO charges have been successfully applied in explaining various experimental data.³⁰ The inconsistency is probably caused by the fact that pK_a^1 values are calculated in aqueous solution and influenced by solvent; however NBO charges are calculated in gas phase. NBO charges might be more accurate indicator than pK_a values to predict the coordination ability of the ligands since it is a property of the ligand itself, while pK_a value calculations involve the solvation energy calculation of the conjugated acid of the ligand. Further experimental evidence is required to verify whether this is true.

Compared with pK_a^1 values, NBO charges are quite close with each other. Thus, pK_a^1 values might be a more sensitive indicator than NBO charges when comparing coordination abilities of the ligands of the same type. When there are nonequivalent coordinating atoms, the NBO charges might indicate which atom is more likely to interact with metal ions to form a stronger M-X bond. The calculated pK_a^1 values are consistent with Hammett substituent constants.³¹ For example, replacing the H ($\sigma_m = 0$) in *m*-BDC (No. 4) with the COOH ($\sigma_m = 0.37$) (No.32 BTC) led to a smaller pK_a^1 value.

3.4 The application of the calculated results

3.4.1 The effect of bond strength on water stability of MOFs

Willis et al.⁹ proposed that PCPs containing 6-coordinate metal ions tend to be more stable than those containing 4-coordinate metal ions, which have more space for water attacks. However, we found Zn(trans-pda) (pda: 1,4-phenylenediacetate) (**1**) which contains 4-coordinated Zn²⁺ and was first synthesized by Liu et al.³² is stable in water as shown in Fig. 3, much more stable than MOF-5 which is built with Zn²⁺ and the BDC²⁻.

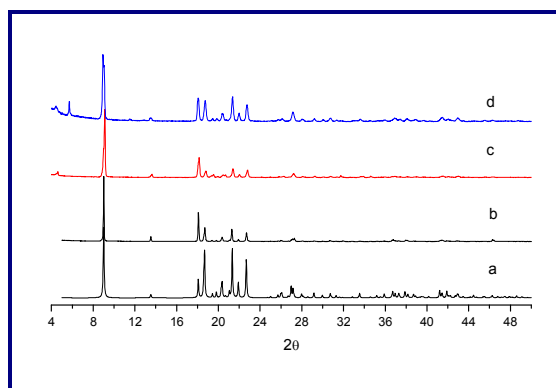


Fig. 3 Powder XRD patterns for **1**: (a) simulated based on the single-crystal structure, (b) as-synthesized, (c) exposed in the air for 7 days and (d) soaked in water for 7 days.

Our calculations found the pK_a^1 of H_2pda (8.81) are larger than that of H_2BDC (5.34), the NBO charges of the O atoms of the pda^{2-} are -0.802 and -0.806, which is also greater than those of the H_2BDC (-0.798) (Fig. 4). Thus both pK_a^1 values and NBO charges indicate that pda^{2-} have stronger coordination ability, forming stronger M-L bonds. This is reasonable because H_2pda , compared to the H_2BDC , introduces the methylene groups, thus destroys the conjugacy. As a result, it has a lower acidity, and its conjugate base should have a higher coordination ability. Thus, our calculated results are consistent with the experimental results. The above results demonstrated that M-X bond strength can alter the general trend that that MOFs containing 6-coordinate metal ions tend to be more stable than those containing 4-coordinate metal ions, again indicating the importance of M-X bond in determining the hydrothermal stability of the MOFs. Willis et al.⁹ also conclude that M-X bond strength is one of the major factors in determining the hydrothermal stability of the PCPs.

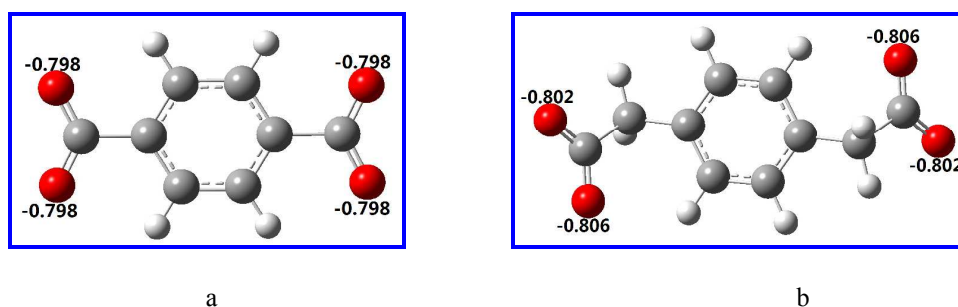


Fig. 4 The NBO charges of the coordinated atoms of a) BDC^{2-} and b) pda^{2-}

3.4.2 Surface properties (hydrophilic or hydrophobic) and steric effect on water stability of MOFs

Walton group's study¹⁰ proposed the incorporation of polar functional groups (e.g., nitro, bromo, chloro, hydroxy, etc.) on the BDC²⁻ linker renders these MOFs more water unstable compared to the parent MOF. On the other hand, placing nonpolar groups (e.g., methyl) on the BDC²⁻ ligand results in structurally robust MOFs. We calculated the BDC²⁻ ligands with two chloro (1.83; -0.763, -0.779), one nitro (1.69; -0.777, -0.789), one bromo (1.83, -0.769, -0.793), and one hydroxyl (4.79, -0.784, -0.798) substituent group and found both the NBO charges and the pK_a¹ values of the conjugated acids of these ligands are smaller than those values of the BDC²⁻ (5.34, -0.798), suggesting lower electron densities on the coordinated atoms. Therefore we think the reason that these MOFs are less water stable than the parent MOF is also likely due to weaker M-L bonds. However, isotypic DMOF-A (9,10-anthracenedicarboxylic acid (ADC): 3.96, -0.786) and DMOF-TM2 (BDC-(CH₃)₄ ligand (Table 3): 6.74, -0.787) are more stable than parent MOF, although the pK_a¹ and NBO charges of ADC and BDC-(CH₃)₄ are not all greater than those values of BDC²⁻. Thus, their stability is due to the surface properties of these MOFs, which are more hydrophobic as proposed by Walton et al.¹⁰ Polar ligands will make the surface more hydrophilic, and will attracting H₂O into the pores causing damage to the framework. The experimental and molecular simulation work done by Walton's group^{17b} later also showed the nonpolar substituents close to carboxylate group not only make the surface hydrophobic, but also shield the carboxylate oxygen-M bonds from the attack of water, thus contributing to the kinetic stability of MOF materials.

Li et al.³³ demonstrated that the methyl groups at the ortho-positions of the coordinating nitrogen atoms of 4,4'-bipyridine will be more stable than that at the meta-positions, which is attributed to the shielding effect of ortho-position methyl groups. Our calculated results (No.29 and No.30 in Table 3) found that the NBO charges (-0.461) of the former is significantly larger than that of the latter (-0.447), also leading to stronger M-L bonds, indicating thermodynamic stability could also exist in this case.

3.4.3 The effect of pore size on hydrothermal stability of MOFs

IRMOF-1 (also called MOF-5) and IRMOF-10 are isotypic with different organic ligands (BDC = 1,4-benzenedicarboxylate for the former, BPDC = 4,4'-biphenyldicarboxylate for the latter). Han et al.³⁴ found the water stability of IRMOF-10 is

weaker than that of IRMOF-1 and thought the reason is due to the bigger pore size. Since pores of both IRMOF-1 and IRMOF-10 are big enough for the access of H₂O molecules and our calculated results found Both the pK_a¹ values of H₂BPDC and NBO charges of the carboxylate-oxygens (No. 20 of Table 1: 3.91, -0.788) are smaller than those of H₂BDC and BDC (No. 1 of Table 1: 5.34, -0.798), we think the reason of the weaker water stability of IRMOF-10 might be due to weaker M-O bonds. The effect of pore size on the water stability of MOFs is yet to be demonstrated. If the pore sizes are too small for water molecules to enter, whether the MOFs can be still destroyed, starting from the surfaces?

3.4.4 Other potential applications of the calculated NBO and pK_a¹ values

By applying the data in Table 3, it is possible to change a water-unstable MOF to a water-stable MOF by replacing the original ligand with a ligand with stronger coordination ability. Long et al.³⁵ applied the tetrazole ligand H₃BTT (No. 50 in Table 3) and synthesized a Cu²⁺ MOF H[Cu(DMF)₆][(Cu₄Cl)₃(BTT)₈-(H₂O)₁₂]·3.5HCl·12H₂O·16CH₃OH (Cu-BTT) (**2**), which have good hydrogen storage property, but water unstable. Our calculated results (Table 3) indicate that the pK_a¹ values of polyazoles decrease in the following order: pyrazole (pK_a¹: 18.06-18.43) ≅ imidazole (16.77-18.74) > triazole (11.10-11.51) > tetrazole (5.65). The same group³⁶ later applied the H₃BTTri (No. 48 in Table 3) triazole ligand and did synthesized an isomorphous structure of **2** {H₃[(Cu₄Cl)₃(BTTri)₈-(DMF)₁₂]·7DMF·76H₂O (**3**)}, which is stable after soaking the solid for 3 days in boiling water or 1 day in a HCl solution (pH=3) and have fairly good hydrogen storage capacity, consisting with our calculated results. Thus, it is possible to turn a water unstable MOF but having a high hydrogen storage property into a water stable MOF with similar hydrogen storage capacity by choosing ligands with stronger coordination ability to form stronger M-X bonds.

The NBO charges of the coordinating atoms of polyazolate ligands of the same triangular geometry (e.g. 51,50,59, 61) decrease in the following order: imidazolate (51:-0.583,-0.636) > pyrazolate (50: -0.424) > triazolate (59: -0.223 (N2), -0.412 (N3); Triazolates tend to coordinate with N2 and N3, not N1.³⁶) > tetrazolate (61: -0.215 (N2); Tetazolates tend to coordinate with N2, not N1.^{35,37}), consisting with the pK_a¹ orders. The NBO charges of 10-13 also predict the same order of coordination ability of these polyazoles. Thus, the NBO charge results suggest that imidazolate MOFs might be more stable than pyrazolate MOFs due to

stronger M-L bonds. This is yet to be verified by experimental evidence.

Our calculated pKa results can help to choose suitable synthetic conditions for MOFs. We know that the pKa of 1,4-cyclohexanedicarboxylic acid (7.36) is greater than H₂BDC, that is to say, the deprotonation is more difficult. Thus a base might be needed to promote the deprotonation. As a fact, most of the MOFs synthesized by 1,4-cyclohexanedicarboxylic acid often require a base in their syntheses.³⁸

3.4.5 The effect of bond polarity on water stability of MOFs

Our calculations (No. 26-52 in Table 3) found the pK_a of polyazolate heterocycles (about 10-20) are much larger than the carboxylic acids (about 4-8). But the NBO charges of polyazolate heterocycles and other N-containing ligands (0.20-0.65) are smaller than those of the carboxylates (about 0.7-0.9). In addition the radius of N is smaller than O due to smaller electronegativity. These two pieces of evidence suggest the bond formed by polyazolate heterocycles is likely weaker than that formed by the carboxylates. The corresponding energy for Cu–O bonds (O is from CO₂⁻ group) is 370 kJ mol⁻¹.³⁹ In contrast, Yaghi et al.³⁹ estimated from the heats of formation of ammoniates such as CuCl·3NH₃ and CuCl₂·2NH₃ that the energy of the Cu(I)–N coordination bond is about 55 kJ mol⁻¹ and the Cu(II)–N bond is about 90 kJ mol⁻¹. Tan and coworkers⁴⁰ also found experimental evidence that M–O (O is from CO₂⁻) is stronger than the M–N (N is from a neutral N-heterocycle). Landis and co-workers^{28c} have used the B3LYP functional and ab initio methods to evaluate “valency-saturated” HnM–X (M: all transition metals) bond enthalpies. They found that the general bond enthalpy ordering of M–X consisted of X = NH₂ < OH. Others also found the bond enthalpies of M–OR are stronger than those of M–NR₂ by theoretical calculation^{28d} or experimental studies.²⁷⁻²⁸ Thus, one should not use pKa values to compare the coordination ability of different class of ligands. The high water stability of those polyazolate MOFs⁴¹ might be due to the lower polarity of the M–N bonds than M–O bonds due to the higher electronegativity of O than that of N, which is also reflected in their NBO charges as higher charges were found on O atoms than on N. We predict under anhydrous condition the thermal stabilities of the MOFs of those ligands are likely inferior to the MOFs synthesized by carboxylate ligands due to weaker bonds.

Chabal et al.⁴² studied the moisture stability of paddle wheel frameworks M(bdc)(ted)_{0.5} [M = Cu, Zn, Ni, Co; bdc = 1,4-benzenedicarbox-ylate; ted = triethylenediamine]. IR

spectroscopy data indicate that a hydrolysis reaction of water molecules with Cu–O–C is observed in the case of Cu(bdc)(ted)_{0.5}. Displacement reactions of ted linkers by water molecules are identified with Zn(bdc)(ted)_{0.5} and Co(bdc)(ted)_{0.5}. In contrast, Ni(bdc)(ted)_{0.5} is less susceptible to reaction with water vapors than the other three compounds. Their study indicates that M-N bonds are not always more water stable than M-O bonds and the water stability of a MOF is affected by both M-L bond polarity and strength. Stronger and less polar M-L bond is favorable for the water stability of a MOF material.

To synthesize a water-stable MOF, if the ligand does not have a big NBO charges, one can choose a suitable metal ion to compensate this. For example, BDC²⁻ may not form water stable MOFs with Zn²⁺ (e.g. MOF-5 is water unstable), but it can form a water stable MOF with Al(III) and Cr(III) (MIL-53(Al or Cr)). Based on experimental evidence, it seems that a very stable ionic bond (Al-O, Zr-O, or Cr-O) cannot be destroyed by the attacks of water molecules under normal conditions. However, if the ionic bond is not very strong, the bond is vulnerable to the attacks of the polar water molecules.

3.4.6 Limitations

Pka¹ values of the same type of ligands can be used to predict the relative coordination ability, but not between different types. However, NBO charges might be able to be used to compare the coordination ability of different type of ligands as indicated in Section 3.4.5.

The pka¹ values are calculated in aqueous solution, NBO charges are calculated in gas phase. However, in reality, the solvent could be something other than H₂O, or mixture of solvents. This could cause some error in predicting the relative coordination ability of these ligands. For example, the NBO charges predict that the N1 in the imidazolate ligand No.51 would tend to coordinate with metal instead of N2 due to its high electron density (-0.636 versus -0.582). In a mixture solvent of DMF and H₂O, it tends to coordinate through N2; however in aqueous ammonia, N1 was coordinated with the metal, not N2.⁴³ This suggests the coordination ability can be varied by solvent effects.

The electron density on the neighboring atoms could also affect the M-X bonds formed, which have not been considered in order to simplify the situations. We include all the NBO charges of these structures in Supporting Information. Metal ions might not choose the atoms having more electron density due to steric effect. For example, we calculated the tetrazole

ligand No. 61 of Table 1 and found N1 (-0.389) would have more electron density than N2 (-0.215). However, metals were found to coordinate with N2 instead of N1 likely due to steric effect.^{35,37} When chelating coordination mode (η^2) can be formed with metal cation due to the ligand structures (e.g. 2-tetrazole pyrimidine⁴⁴ and N,N,N-Tris-tetrazol-5-yl-amine⁴⁴), N1 participate in the coordination, not N2. η^2 -coordination mode is preferred to η^1 coordination mode due to chelating effect.

There are quite a few resonance structures possible for the polyazolate structures, but we only calculated the NBO charges of the most stable states (the delocalized form) of the deprotonated ones. After coordination, the electron density would not be delocalized, but localized. The final electron densities provided to the metal ions from the coordinating atoms might be different from the calculated NBO charges.

3.4.7 Other factors on hydrothermal stability of MOFs

We are aware other factors other than the above mentioned ones could affect the water stability of MOFs. As Han et al.³⁴ proposed that a Zn ion forms four Zn–O bonds in IRMOF-1 and IRMOF-10, whereas a Zn in MOF-74 has five Zn–O bonds. Therefore, it is expected that more H₂O molecules will be involved in the dissociation of MOF-74 than IRMOF-1 and IRMOF-10. In addition, the fused and infinite helical SBUs in MOF-74 support the framework structure more strongly than the isolated ones in IRMOF-1 and IRMOF-10. Willis et al.⁹ also found the structure of SBUs have influence on the hydrothermal stability of MOFs.

Costantino et al.⁴⁵ found tubular MOFs based on copper (II) phosphinates and bipyridine can be highly stable in water. However, the possibility to form more dense and stable phases could affect their water stability, leading to slow and spontaneous transformations driven by the hydrolysis of the M-X bonds.

Jhung et al.⁴⁶ found chemical stability to acids, bases, and water decreases in the order of Cr-BDC > Al-BDC > V-BDC, suggesting stability increases with increasing the inertness or lability of the central metal ions. However, thermal stability decreases in the order of Al-BDC > Cr-BDC > V-BDC, and this tendency was explained by the strength of the M-O bond in common oxides like Al₂O₃, Cr₂O₃, and V₂O₅.⁴⁶ They also notify others that in order to evaluate precisely the stability of a MOF, it is necessary to remove uncoordinated organic

linkers that are located in the pores of the MOF, because a filled MOF may be more stable than the same MOF after purification.

It is well-known that most MOFs with ultralarge solvent cavities are extremely unstable when solvent being removed via conventional drying process due to the elimination of surface tension upon removal of the solvent.⁴⁷ Supercritical processing using CO₂ has been shown to be able to solve this problem.⁴⁸

Usually stronger bonds would result in better thermal stability.^{49,9} And generally the thermal stability of flexible structures is less than that of rigid ones.⁵⁰ Mu and Walton⁵¹ found that the thermal stability of MOFs is determined by the coordination number and local coordination environment instead of framework topology.

4. Conclusion

We systematically calculated NBO charges (gas phase) and/or the pK_a¹ values (in aqueous solution, conjugated acids of the ligands) of 32 multicarboxylate ligands and 31 N-containing heterocyclic ligands using DFT at 298.15 K at the B3LYP/6-31+G(d,p) level of theory. These values are inherent properties of these ligands, which should be useful for design purposes. We demonstrated that pK_a¹ values and NBO charges have predicting values for judging relative coordination abilities of the N-containing and carboxylate ligands by successfully applied them to explain the water stability of MOFs.

Kinetic stable MOFs could eventually be destroyed over long period of time. It is better to make thermodynamically stable MOFs, which should have very strong M-L bonds. To form a MOF of high hydrothermal stability, we recommend that ligands with high coordination ability and metal ions of small radii and high charges be used. To synthesize a water-stable MOF, if a ligand does not have high NBO charges, one can choose a suitable metal ion to compensate this. For example, BDC²⁻ may not form water stable MOFs with Zn²⁺ (e.g. MOF-5 is water unstable), but it can form a water stable MOF with Al(III) and Cr(III) (MIL-53(Al or Cr)) due to the higher charges of the metal ion. Based on experimental evidence, it seems a very strong bond (Al-O, Zr-O, or Cr-O) cannot be destroyed by the attacks of water under normal conditions although these bonds are polar.

Many MOFs were synthesized without reporting their water stability. Based on our calculated results which can be easily extended using the easy and not costly calculation method, it is possible to predict their water stability so that some of them can be selected for hydrogen storage applications.

Acknowledgements

We thank National Natural Science Foundation of China (Project 21171095, 21071082, 21103093), the Natural Science Foundation of Education Department of Jiangsu Province (No. 13kjb150022), and the Priority Academic Program Development of Jiangsu Higher Education Institutions (PAPD) for their support for our work.

5. Notes and references

- (1) (a) Satyapal, S.; Petrovic, J.; Read, C.; Thomas, G.; Ordaz, G. *Catal. Today* **2007**, *120* (3-4), 246-256; (b) Park, N.; Choi, K.; Hwang, J.; Kim, D. W.; Kim, D. O.; Ihm, J. *PANS* **2012**, *109* (49), 19893–19899; (c) McWhorter, S.; Read, C.; Ordaz, G.; Stetson, N. *Curr. Opin. Solid State Mat. Sci.* **2011**, *15* (2), 29-38; (d) Jena, P. *J. Phys. Chem. Lett.* **2011**, *2* (3), 206-211; (e) Eberle, U.; Felderhoff, M.; Schüth, F. *Angew. Chem. Int. Ed.* **2009**, *48* (36), 6608-6630.
- (2) (a) Dibandjo, P.; Zlotea, C.; Gadiou, R.; Ghimbeu, C. M.; Cuevas, F.; Latroche, M.; Leroy, E.; Vix-Guterl, C. *Int. J. Hydrog. Energy* **2013**, *38* (2), 952-965; (b) Suh, M. P.; Park, H. J.; Prasad, T. K.; Lim, D. W. *Chem. Rev.* **2012**, *112* (2), 782-835; (c) Bastos-Neto, M.; Patzschke, C.; Lange, M.; Mollmer, J.; Moller, A.; Fichtner, S.; Schrage, C.; Lassig, D.; Lincke, J.; Staudt, R.; Krautscheid, H.; Glaser, R. *Energy Environ. Sci.* **2012**, *5* (8), 8294-8303; (d) Sculley, J.; Yuan, D.; Zhou, H.-C. *Energy Environ. Sci.* **2011**, *4* (8), 2721-2735; (e) Hirscher, M. *Angew. Chem. Int. Ed.* **2011**, *50* (3), 581-582; (f) Zhao, D.; Yuan, D. Q.; Zhou, H. C. *Energy Environ. Sci.* **2008**, *1* (2), 222-235; (g) Murray, L. J.; Dinca, M.; Long, J. R. *Chem. Soc. Rev.* **2009**, *38* (5), 1294-1314; (h) Ferey, G. *Chem. Soc. Rev.* **2008**, *37* (1), 191-214; (i) Rowsell, J. L. C.; Yaghi, O. M. *Angew. Chem. Int. Ed.* **2005**, *44* (30), 4670-4679.
- (3) (a) Ding, F.; Yakobson, B. I. *Front. Phys.* **2011**, *6*, 142-150; (b) Wang, L. F.; Yang, R. T. *Catal. Rev. -Sci. Eng.* **2010**, *52* (4), 411-461; (c) Wang, L. F.; Yang, R. T. *Energy Environ. Sci.* **2008**, *1* (2), 268-279.
- (4) Hoskins, B. F.; Robson, R. *J. Am. Chem. Soc.* **1989**, *111* (15), 5962-5964.
- (5) Batten, S. R.; Champness, N. R.; Chen, X.-M.; Garcia-Martinez, J.; Kitagawa, S.; Ohrstrom, L.; O'Keeffe, M.; Suh, M. P.; Reedijk, J. *Crystengcomm* **2012**, *14*, 3001-3004.
- (6) (a) Stock, N.; Biswas, S. *Chem. Rev.* **2012**, *112* (2), 933-969; (b) Wang, C.; Zhang, T.; Lin, W. B. *Chem. Rev.* **2012**, *112* (2), 1084-1104; (c) Lan, Y. Q.; Li, S. L.; Jiang, H. L.; Xu, Q. *Chem. Eur. J.* **2012**, *18* (26), 8076-8083; (d) Zhang, Y. B.; Zhou, H. L.; Lin, R. B.; Zhang, C.; Lin, J. B.; Zhang, J. P.; Chen, X. M. *Nature Commun.* **2012**, *3*.
- (7) Küsgens, P.; Rose, M.; Senkovska, I.; Fröde, H.; Henschel, A.; Siegle, S.; Kaskel, S. *Microporous Mesoporous Mat.* **2009**, *120* (3), 325-330.

- (8) (a) Panella, B.; Hirscher, M. *Adv. Mater.* **2005**, *17* (5), 538-541; (b) Huang, L.; Wang, H.; Chen, J.; Wang, Z.; Sun, J.; Zhao, D.; Yan, Y. *Microporous Mesoporous Mat.* **2003**, *58* (2), 105-114.
- (9) Low, J. J.; Benin, A. I.; Jakubczak, P.; Abrahamian, J. F.; Faheem, S. A.; Willis, R. R. *J. Am. Chem. Soc.* **2009**, *131* (43), 15834-15842.
- (10) Jasuja, H.; Huang, Y.-g.; Walton, K. S. *Langmuir* **2012**, *28* (49), 16874-16880.
- (11) Choi, H. J.; Dinca, M.; Dailly, A.; Long, J. R. *Energy Environ. Sci.* **2010**, *3* (1), 117-123.
- (12) Cychoz, K. A.; Matzger, A. J. *Langmuir* **2010**, *26* (22), 17198-17202.
- (13) Cavka, J. H.; Jakobsen, S.; Olsbye, U.; Guillou, N.; Lamberti, C.; Bordiga, S.; Lillerud, K. P. *J. Am. Chem. Soc.* **2008**, *130* (42), 13850-13851.
- (14) Schoenecker, P. M.; Carson, C. G.; Jasuja, H.; Flemming, C. J. J.; Walton, K. S. *Industrial & Engineering Chemistry Research* **2012**, *51* (18), 6513-6519.
- (15) Mohamed, M. H.; Elsaidi, S. K.; Wojtas, L.; Pham, T.; Forrest, K. A.; Tudor, B.; Space, B.; Zaworotko, M. J. *J. Am. Chem. Soc.* **2012**, *134* (48), 19556-19559.
- (16) Glendening, E. D.; Reed, A. E.; Carpenter, J. E.; Weinhold, F., *NBO Version 3.1*.
- (17) (a) Colombo, V.; Galli, S.; Choi, H. J.; Han, G. D.; Maspero, A.; Palmisano, G.; Masciocchi, N.; Long, J. R. *Chem. Sci.* **2011**, *2* (7), 1311-1319; (b) Jasuja, H.; Burtch, N. C.; Huang, Y. G.; Cai, Y.; Walton, K. S. *Langmuir* **2013**, *29* (2), 633-642.
- (18) (a) Zhang, S.; Baker, J.; Pulay, P. *J. Phys. Chem. A* **2009**, *114* (1), 425-431; (b) Zeng, Y.; Chen, X.; Zhao, D.; Li, H.; Zhang, Y.; Xiao, X. *Fluid Phase Equilib.* **2012**, *313* (0), 148-155; (c) Zhang, S.; Baker, J.; Pulay, P. *J. Phys. Chem. A* **2009**, *114* (1), 432-442.
- (19) Zhang, S. *J. Comput. Chem.* **2012**, *33* (31), 2469-2482.
- (20) Ali, S. T.; Karamat, S.; Kona, J.; Fabian, W. M. F. *J. Phys. Chem. A* **2010**, *114* (47), 12470-12478.
- (21) Lee, T. B.; McKee, M. L. *Phys. Chem. Chem. Phys.* **2011**, *13* (21), 10258-10269.
- (22) Marenich, A. V.; Cramer, C. J.; Truhlar, D. G. *J. Phys. Chem. B* **2009**, *113* (18), 6378-6396.
- (23) (a) Ho, J. M.; Coote, M. L. *Theor. Chem. Acc.* **2010**, *125* (1-2), 3-21; (b) Sadlej-Sosnowska, N. *Theor. Chem. Acc.* **2007**, *118* (2), 281-293.
- (24) (a) Liptak, M. D.; Shields, G. C. *J. Am. Chem. Soc.* **2001**, *123* (30), 7314-7319; (b) Sutton, C. C. R.; Franks, G. V.; da Silva, G. *J. Phys. Chem. B* **2012**, *116* (39), 11999-12006.
- (25) Namazian, M.; Zakery, M.; Noorbala, M. R.; Coote, M. L. *Chem. Phys. Lett.* **2008**, *451* (1-3), 163-168.
- (26) Fleming, I., *Frontier orbitals and Organic Chemical Reactions*. John Wiley & Sons: New York, 1976.
- (27) Holland, P. L.; Andersen, R. A.; Bergman, R. G.; Huang, J.; Nolan, S. P. *J. Am. Chem. Soc.* **1997**, *119* (52), 12800-12814.
- (28) (a) Schock, L. E.; Marks, T. J. *J. Am. Chem. Soc.* **1988**, *110* (23), 7701-7715; (b) Bryndza, H. E.; Fong, L. K.; Paciello, R. A.; Tam, W.; Bercaw, J. E. *J. Am. Chem. Soc.* **1987**, *109* (5), 1444-1456; (c) Uddin, J.; Morales, C. M.; Maynard, J. H.; Landis, C. R. *Organometallics* **2006**, *25* (23), 5566-5581; (d) Devarajan, D.; Gunnoe, T. B.; Ess, D. H. *Inorg. Chem.* **2012**, *51* (12), 6710-6718.
- (29) Foresman, J. B.; Frisch, A. E., *Exploring Chemistry With Electronic Structure Methods*. Gaussian Inc.: Pittsburgh, PA, 1998.
- (30) (a) Hargis, J. C.; White, J. K.; Woodcock, H. L. *Abstracts of Papers of the American Chemical Society* **2012**, *244*; (b) Hernandez-Rivera, S. P.; Infante-Castillo, R. *Comput. Theor. Chem.* **2011**, *963* (2-3), 279-283; (c) Hernandez-Rivera, S. P.; Infante-Castillo, R. *Theochem-J. Mol. Struct.* **2010**, *960* (1-3), 57-62; (d) Chojnacki, J. *Polyhedron* **2008**, *27* (3), 969-976.
- (31) Hansch, C.; Leo, A.; Taft, R. W. *Chem. Rev.* **1991**, *91*, 165-195.
- (32) Liu, T.; Lü, J.; Shi, L.; Guo, Z.; Cao, R. *Crystengcomm* **2009**, *11* (4), 583.

- (33) Ma, D. Y.; Li, Y. W.; Li, Z. *Chem. Commun.* **2011**, 47 (26), 7377-7379.
- (34) Han, S. S.; Choi, S. H.; van Duin, A. C. T. *Chem. Commun.* **2010**, 46 (31), 5713-5715.
- (35) Dincă, M.; Han, W. S.; Liu, Y.; Dailly, A.; Brown, C. M.; Long, J. R. *Angew. Chem. Int. Ed.* **2007**, 46 (9), 1419-1422.
- (36) Demessence, A.; D'Alessandro, D. M.; Foo, M. L.; Long, J. R. *J. Am. Chem. Soc.* **2009**, 131 (25), 8784-8786.
- (37) Pachfule, P.; Banerjee, R. *Cryst. Growth Des.* **2011**, 11 (12), 5176-5181.
- (38) (a) Li, T.; Huang, X. H.; Zhao, Y. F.; Li, H. H.; Wu, S. T.; Huang, C. C. *Dalton Trans.* **2012**, 41 (41), 12872-12881; (b) Rao, K. P.; Thirumurugan, A.; Rao, C. N. R. *Chem. Eur. J.* **2007**, 13 (11), 3193-3201; (c) Dong, L.-N.; Tian, Y.; Li, X.; Jiang, Y. *J. Coord. Chem.* **2010**, 63 (12), 2088-2096.
- (39) Yaghi, O. M.; O'Keeffe, M.; Ockwig, N. W.; Chae, H. K.; Eddaoudi, M.; Kim, J. *Nature* **2003**, 423 (6941), 705-714.
- (40) Chen, Z.; Wang, G.; Xu, Z.; Li, H.; Dhôtel, A.; Zeng, X. C.; Chen, B.; Saiter, J.-M.; Tan, L. *Adv. Mater.* **2013**, 25 (42), 6106-6111.
- (41) (a) Huang, X.-C.; Lin, Y.-Y.; Zhang, J.-P.; Chen, X.-M. *Angew. Chem. Int. Ed.* **2006**, 45 (10), 1557-1559; (b) Liu, Y.; Kravtsov, V. C.; Larsen, R.; Eddaoudi, M. *Chem. Commun.* **2006**, 0 (14), 1488-1490.
- (42) Tan, K.; Nijem, N.; Canepa, P.; Gong, Q.; Li, J.; Thonhauser, T.; Chabal, Y. J. *Chem. Mater.* **2012**, 24 (16), 3153-3167.
- (43) Chen, S.-S.; Chen, M.; Takamizawa, S.; Wang, P.; Lv, G.-C.; Sun, W.-Y. *Chem. Commun.* **2011**, 47 (17), 4902-4904.
- (44) Pachfule, P.; Das, R.; Poddar, P.; Banerjee, R. *Cryst. Growth Des.* **2010**, 10 (6), 2475-2478.
- (45) Taddei, M.; Ienco, A.; Costantino, F.; Guerri, A. *Rsc Adv.* **2013**, 3 (48), 26177-26183.
- (46) Kang, I. J.; Khan, N. A.; Haque, E.; Jung, S. H. *Chem. Eur. J.* **2011**, 17 (23), 6437-6442.
- (47) Song, X.; Oh, M.; Lah, M. S. *Inorg. Chem.* **2013**, 52 (19), 10869-10876.
- (48) Nelson, A. P.; Farha, O. K.; Mulfort, K. L.; Hupp, J. T. *J. Am. Chem. Soc.* **2008**, 131 (2), 458-460.
- (49) Liang, Z.; Marshall, M.; Chaffee, A. L. *Microporous Mesoporous Mat.* **2010**, 132 (3), 305-310.
- (50) (a) Hou, C.; Liu, Q.; Wang, P.; Sun, W. Y. *Microporous Mesoporous Mat.* **2013**, 172, 61-66; (b) Liu, G.-Z.; Xin, L.-Y.; Wang, L.-Y. *Crystengcomm* **2011**, 13 (8), 3013-3020.
- (51) Mu, B.; Walton, K. S. *J. Phys. Chem. C* **2011**, 115 (46), 22748-22754.

The pK_a^1 values and NBO charges of 31 carboxylate ligands and 27 N-heterocyclic ligands were calculated at 273.15 K with B3LYP/6-31+G(d,p) level of calculations, which are useful to understand the water and thermal stability of Metal-Organic Frameworks (MOFs).

